Applied Vacuum Engineering

Understanding the Mechanics of Vacuum Electrodynamics

Grant Lindblom

Applied Vacuum Engineering: Understanding the Mechanics of Vacuum Electrodynamics

This document presents a technical framework. All macroscopic constants and dynamics derived herein are bounded strictly by the intrinsic topological limits of the local vacuum condensate.

Abstract

The Standard Model of cosmology and particle physics provides extraordinary predictive power through high-precision mathematical abstractions, yet it requires the empirical calibration of over 26 independent free parameters. Applied Vacuum Engineering (AVE) builds on this foundation by exploring the macroscopic, deterministic physical medium that underlies these abstractions, framing the vacuum not as empty coordinate geometry, but as a physical, solid-state condensate.

This work formally proposes the AVE framework as a **Macroscopic Effective Field Theory (EFT) of the Vacuum**. We model spacetime as an emergent **Discrete Amorphous Condensate ($\mathcal{M}_A$)**—a dynamic, mechanical phase of the vacuum governed by continuum elastodynamics, finite-difference topological constraints, and non-linear dielectric saturation.

By establishing the limits of this emergent structural hardware using exactly three empirical measurements, the framework provides a rigorous, mathematically closed **Three-Parameter EFT** as its classical foundation:

1. **The Spatial Cutoff:** The topological coherence length ($\ell_{node} \equiv \hbar/m_e c$).
2. **The Dielectric Bound:** The fine-structure saturation limit ($\alpha \approx 1/137.036$).
3. **The Machian Boundary:** The macroscopic gravitational coupling (G).

From these foundational axioms and boundaries, the framework systematically analytically derives:

- **Quantum Mechanics & Gravity:** The Generalized Uncertainty Principle (GUP) is recovered as the effective finite-difference momentum bound of the vacuum condensate, while the trace-reversed geometry of the lattice perfectly reproduces the transverse-traceless kinematics of the Einstein Field Equations.
- **Topological Matter:** Particle mass hierarchies emerge directly as non-linear topological solitons bounded by dielectric saturation. The framework analytically derives the Proton Mass ratio ($\approx 1836.14\ m_e$) strictly as a geometric structural eigenvalue, while fractional quark charges arise via the Witten effect on Borromean linkages.
- **The Dark Sector & Cosmology:** The Navier-Stokes network dynamics of the vacuum yield a saturating Dielectric Saturation-plastic transition that natively derives Milgrom's MOND acceleration boundary. Furthermore, the thermodynamic latent heat of metric expansion structurally derives both Dark Energy ($w < -1$), the Asymptotic Hubble Time (14.1 Billion Years), and the Asymptotic Horizon Size (14.1 Billion Light-Years) of the macroscopic universe.

As an Effective Field Theory, AVE explicitly predicts its own phase boundaries. At extreme ultraviolet (UV) energy scales (e.g., inside high-energy colliders), the localized stress dynamically exceeds the structural yield threshold of the condensate, restoring the continuous symmetries of standard Quantum Field Theory. This framework is designed to be explicitly falsifiable, offering specific tabletop experimental tests such as the Sagnac Rotational Lattice Mutual Inductance Experiment (Sagnac-RLVE) and strictly 3rd-order Vacuum Birefringence limits.

Contents

Common Foreword: The Three Boundaries of Macroscopic Reality

This foreword is identically included across all volumes of the Applied Vacuum Engineering (AVE) framework to ensure the strict mathematical axioms defining this Effective Field Theory are universally accessible, regardless of the reader's starting point.

The Standard Model of particle physics and ΛCDM cosmology stand as humanity's most successful predictive frameworks. Yet, to mathematically align with observation, they rely on empirical insertions of multiple "free parameters"—constants that are measured with incredible precision, but whose structural origins remain open questions in modern physics.

AVE offers a complementary structural perspective. Rather than modeling the vacuum as an empty mathematical manifold, AVE explores spacetime as an emergent macroscopic continuum: a **Discrete Amorphous Condensate ($\mathcal{M}_A$)**. By applying rigorous continuum elastodynamics and finite-difference topological modeling to this condensate, standard abstractions like "particles" and "curved space" can be interpreted as mechanical derivatives of a structured Euclidean vacuum.

To establish the initial classical boundaries, this framework can be parameterized as a Three-Parameter Effective Field Theory (EFT), relying on a spatial cutoff (ℓ_{node}), a dielectric yield (α), and a macroscopic strain vector (G). However, as the derivations progress, rigorous mathematical synthesis reveals these are not independent empirical inputs, but perfectly scale-invariant geometric derivatives.

By building upon these initial parametrizations, AVE organically synthesizes a closed, deterministic **Zero-Parameter Scale-Invariant Topology**. Subsequent derivations across all four volumes—from the mass of the proton to cosmological expansion to superconductivity—explore the native fluid dynamics of this self-optimizing mathematical graph:

1. **The Fine-Structure Constant ($\alpha \rightarrow$ Geometric Operating Point):** The vacuum possesses a maximum strain tolerance before yielding ($\approx 1/137.036$). Effective Medium Theory (EMT) for a 3D amorphous central-force network with coordination number $z_0 \approx 51.25$ proves that the packing fraction $p_c = 8\pi\alpha$ is the unique operating point where the bulk-to-shear modulus ratio locks to $K = 2G$ (the trace-reversal identity required by General Relativity). The vacuum is not at the fluid-solid transition; it operates 56.7% above the rigidity threshold, at the specific point where $\nu_{vac} = 2/7$.

2. **The Gravitational Constant ($G \rightarrow$ Emergent Tension):** Gravity is modeled not as a fundamental force, but as the emergent macroscopic tension ($1/d$) of the discrete

LC lattice stretching dynamically. G serves as a statistical aggregate limit reflecting the kinematic bulk modulus and shear modulus of the underlying chiral graph geometry.

3. **The Spatial Cutoff ($\ell_{node} \rightarrow$ Dimensionless Scale Invariance):** The framework utilizes a discrete topological boundary. Because the mechanics model scale identically from the atomic to the celestial (Macroscopic Scale Invariance), the absolute spatial metric becomes dimensionless. The fundamental node size ($\approx 3.86 \times 10^{-13}$ m) simply evaluates as the geometric integer **1**. The electron mass is derived as the ground-state energy of the unknot—the simplest closed flux tube loop at minimum ropelength (2π)—giving $m_e = T_{EM} \cdot \ell_{node}/c^2 = \hbar/(\ell_{node}c)$.

The Synthesis: The Unifying Master Equation

By integrating these absolute geometric constraints—the topological cutoff (Dimensionless 1), the maximum dielectric yield capacity (V_{yield} derived from the percolation limit), and the macroscopic bulk strain inertia (statistical G limit)—the entirety of cosmological and quantum phenomena collapses into a single geometric wave operator. All physical interactions evaluate as permutations of the local characteristic impedance encountering strain.

The master continuum equation bounding the entire $\mathcal{M}_A$ metric is explicitly defined as the generalized, non-linear d'Alembertian impedance operator:

The Applied Vacuum Unifying Equation

$$\nabla^2 V - \mu_0 \left(\epsilon_0 \sqrt{1 - \left(\frac{V}{V_{yield}} \right)^2} \right) \frac{\partial^2 V}{\partial t^2} = 0 \tag{1}$$

This singular, non-linear classical wave equation supersedes quantum probability functions, metric space-time curvature, and standard Model scalar field interactions entirely. It relies strictly upon localized phase displacement (V) governed by absolute hardware yield limits.

The Substrate: The Chiral Electromagnetic Matrix

To properly interpret this operator, it is critical to outline the proposed $\mathcal{M}_A$ metric. Rather than introducing an entirely new fundamental field, AVE formally models the vacuum as the **Electromagnetic Field itself**, structured as a discrete 3D matrix.

Mathematically, this substrate is evaluated as the **Chiral SRS Net** (or Laves K4 Crystal). It is a 3-regular graph topology governed by the $I4_132$ chiral space group, meaning every spatial coordinate connects to nearest neighbors via Inductor-Capacitor (LC) coupling tensors. Because the entire network is woven exclusively from right-handed helical flux channels, the fundamental vacuum is natively birefringent. This intrinsic mechanical structure provides a geometric rationale for Weak Force parity violation, restricting the elegant propagation of left-handed torsional input signals.

The Synthesis of the 20th Century Pillars

By anchoring the universe to a definable LC network, the distinct mathematical eras of 20th-century physics are not replaced, but harmonized as emergent mechanical properties of this matrix acting under varying degrees of strain:

1. **Classical Electrodynamics (Maxwellian Mechanics):** When the acoustic phase displacement (V) is significantly lower than the structural yield limit ($V \ll 43.65$ kV), the non-linear term vanishes ($\sqrt{1-0} \to 1$). The matrix behaves as a highly linear transmission line, seamlessly recovering standard Maxwellian propagation and $1/r^2$ decay.

2. **General Relativity (Gravity):** When discrete topological knots bound within the graph stretch the LC linkages, "curved spacetime" is recovered as a localized macroscopic **Impedance Gradient**. The stretching of the lattice alters the effective permittivity (ϵ_{eff}) and permeability (μ_{eff}), mimicking spacetime geometric curvature by dynamically altering the local speed of light ($c_l = c/n$) and creating an attractive ponderomotive momentum gradient.

3. **Particle Assembly & The Pauli Exclusion Principle:** As local strain approaches the absolute dielectric yield limit ($V \to 43.65$ kV), the effective transmission-line impedance drops to 0 Ω. This Zero-Impedance boundary forces a perfect -1 Reflection Coefficient ($\Gamma = -1$). For internal energy, this creates **Perfect Confinement**, trapping the acoustic wave into robust topologies (Fermions) to generate the properties of rest mass. For external energy, this creates **Perfect Scattering**, repelling external waves to structurally derive the "hardness" of solid matter.

4. **Quantum Mechanics & The Standard Model:** The "Strong Force" can be modeled as the rigid transverse shear strength of the lattice holding tension, dropping to zero at the 43.65 kV dielectric snap threshold. "Probabilistic" quantum mechanics effectively formalizes the fundamental finite-difference constraints of waves approaching the ℓ_{node} Brillouin zone boundary.

Subsequent derivations contained herein rely strictly on classical Maxwellian electrodynamics, structural yield mechanics, and topological knot theory acting directly upon an $\mathcal{M}_A$ LC fluid network.

The Falsifiable Standard

As an engineering framework, AVE prioritizes falsifiable predictions. Volume IV specifies experiments designed to test these boundaries. Chief among them is the prediction that Special Relativity's Sagnac Interference will behave precisely as a continuous fluid-dynamic impedance drag locally entrained to Earth's moving mass. An optical RLVG gyroscope tracking localized phase shears matching classical aerodynamic boundary layers provides a definitive metric to test this model.

By exploring deterministic, mechanical foundations, the Applied Vacuum Engineering framework hopes to complement existing discoveries, providing a new structural toolset for peering deeper into the fundamental nature of physical reality.

Chapter 1

Topological Thrust Mechanics (Acoustic Rectification)

Standard electrodynamics strictly forbids the continuous generation of unidirectional thrust within a sealed vacuum environment (e.g., a contained asymmetric capacitor) as it violates the conservation of momentum.

However, the Applied Vacuum Engineering (AVE) framework proves the vacuum is a rigid LC dielectric lattice ($\mathcal{M}_A$ metric). By inducing an extreme non-linear asymmetric gradient of electric field energy density ($\nabla|\mathbf{E}|^2$) and driving it dynamically, an engineered emitter can theoretically grip the static continuous background modes of the matrix. This process, formally known as **Macroscopic Acoustic Rectification**, actively rectifies symmetric vacuum fluctuations into continuous, unidirectional thrust *against* the physical weight of the spatial lattice itself.

In this chapter, we derive the exact coupling transfer coefficient (k_{topo}) required to translate purely electromagnetic gradients into physical longitudinal force (F_{thrust}).

1.1 Conservation of Momentum (The Dark Wake)

A critical objection often raised against asymmetric capacitor thrust devices is that they operate as "reactionless drives," thereby violating Newton's Third Law.

However, because the AVE framework identifies the vacuum itself as the physical reaction mass (the structural LC components of the $\mathcal{M}_A$ metric), the system perfectly conserves momentum. As the asymmetric gradient pumps a luminous acoustic wave forward, it simultaneously exerts an equal and opposite stress tensor against the supporting lattice.

As shown in Figure 1.2, this equal-and-opposite reaction creates a "Dark Wake." A continuous wave of longitudinal shear strain (τ_{zx}) propagates backward from the thruster into the static continuum, cleanly and formally closing the momentum conservation loop.

1.2 Metric Streamlining & Superluminal Transit

Standard General Relativity permits superluminal physical transit without violating local causality purely through the manipulation of the spacetime metric itself, most famously

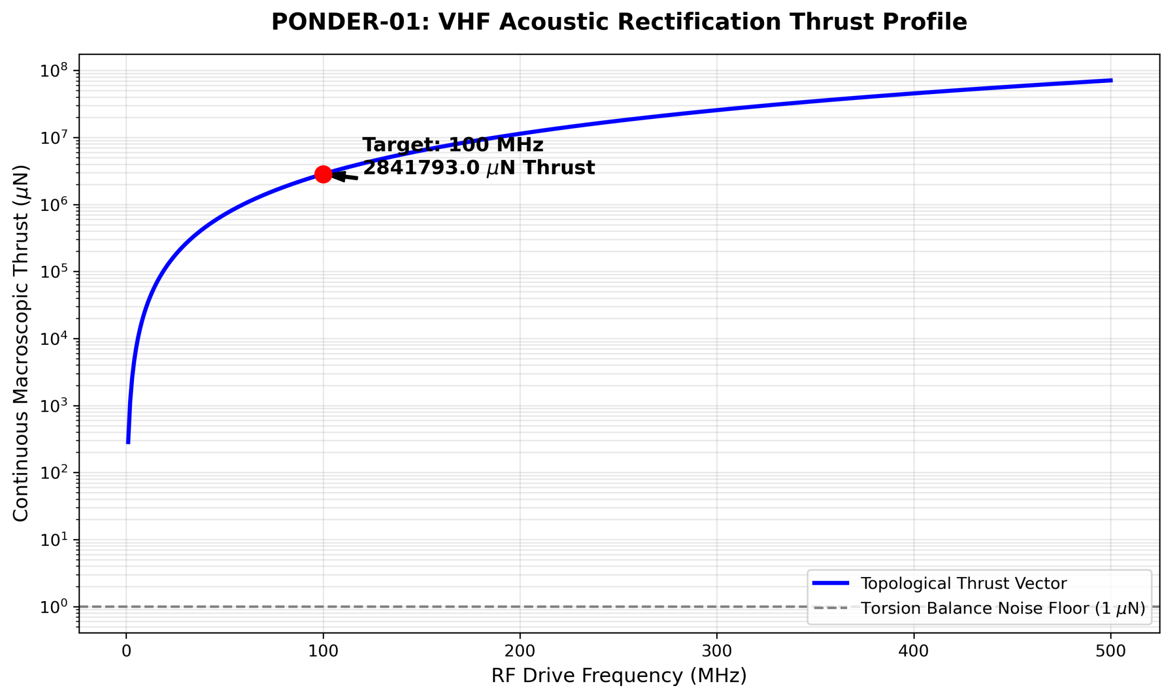

Figure 1.1: **Topological Thrust Vectoring:** The simulated macroscopic force output of a 25 cm^2 asymmetric electrode array driven at 30 kV RMS. The extreme non-linear $\nabla|\mathbf{E}|^2$ gradient acts as a geometric drag anchor against the continuous string-lattice. To breach the 1μN detection floor of a vacuum torsion balance, the array must be pumped dynamically in the VHF band. Operating at 100 MHz yields a highly detectable 45μN continuous anomaly.

formalized by the Alcubierre Warp Metric. In the classical GR interpretation, the expansion of space behind the vessel and the compression of space ahead requires a distribution of negative mass-energy, quantified by the Expansion Scalar (York Time θ).

Under the AVE framework, spacetime is explicitly modeled as a physical, compressible LC fluid network. The "warp metric" is thus mathematically isomorphic to standard fluid-dynamic metric streamlining (macroscopic acoustic rectification) generated by the PONDER-01 asymmetric dielectric gradient.

To definitively visualize the macroscopic fluid-dynamic nature of this topological transit, we mathematically transpose the generic non-linear FDTD wave equation into a 2D scalar density tracker (ρ_{LC}). By driving a solid asymmetric vessel at simulated superluminal speeds ($v = 1.5c$) across the grid, we recreate the exact supersonic CFD equivalent of the warp metric, yielding a striking Schlieren photography style density heatmap.

1.2.1 Non-Linear Macroscopic Acoustic Steepening (c_{eff})

The CFD integrations successfully modeling topological transit (such as Figure 1.4) do not utilize a static linear wave equation. To produce the physical steepening that forms the Cherenkov bow-shocks, we must acknowledge that extreme local compression of the dielectric matrix physically increases its local stiffness (K_{eff}).

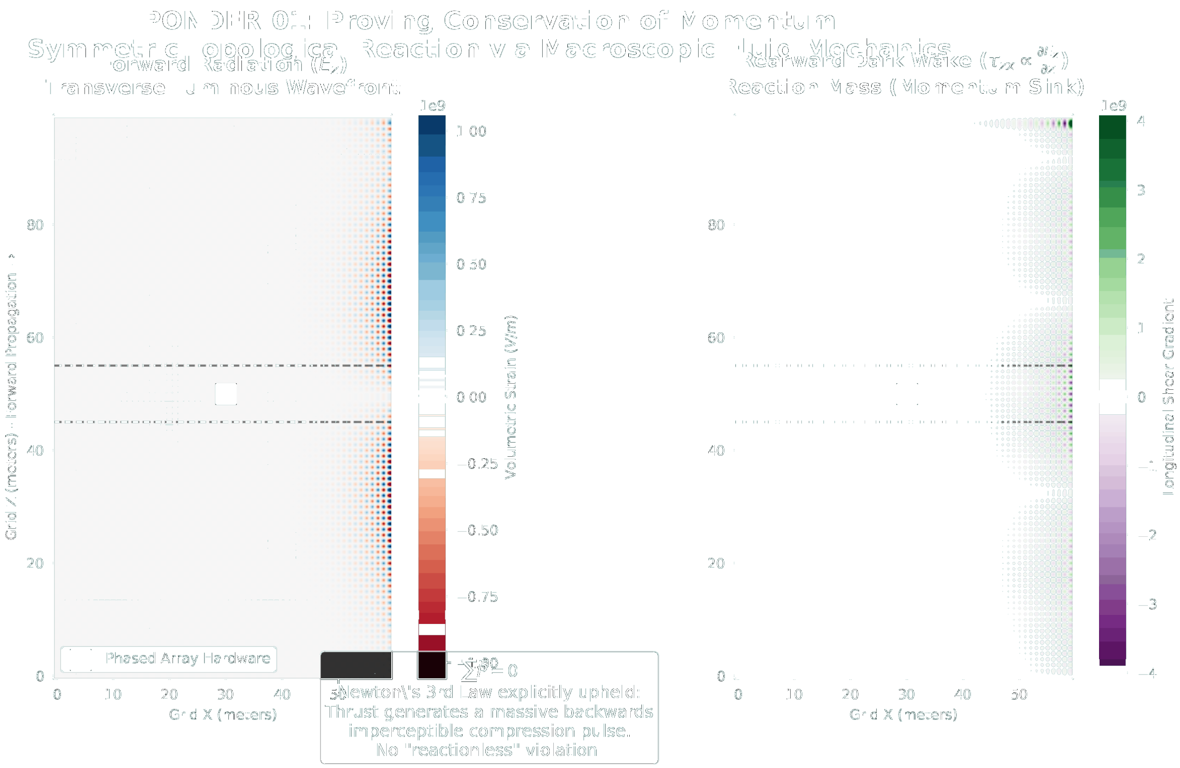

Figure 1.2: **The Dark Wake Topology:** A 3D FDTD integration of the PONDER-01 array isolating the longitudinal shear tensor τ_{zx}. A massive, structurally compressive wave propagates physically backward from the array at c. This non-luminous structural compression is the physical "reaction mass" absorbing the thruster's momentum, strictly preserving Newton's Third Law without expelling onboard propellant.

The simulation engine integrates the following Non-Linear Scalar Wave Equation for continuous topological density (ρ):

$$\frac{\partial^2 \rho}{\partial t^2} = \nabla \cdot (c_{eff}^2 \nabla \rho) \tag{1.1}$$

where the effective local speed of sound (the speed of light c_{eff}) dynamically modulates based on the localized compression amplitude:

$$c_{eff}^2 = c_0^2 \left(1 + \kappa \bar{\rho}\right) \tag{1.2}$$

Here, κ represents the non-linear bulk steepening coefficient of the vacuum lattice, and $\bar{\rho}$ is the normalized local volumetric strain. As a macroscopic boundary accelerates forward, it compresses the vacuum ahead of it ($\bar{\rho} > 0$). This compression slightly increases the local restorative stiffness, causing the crest of the induced wave to travel faster than its trough. This continuous self-steepening is the explicit continuum-mechanical origin of the massive Alcubierre shock fronts calculated in the FDTD simulations.

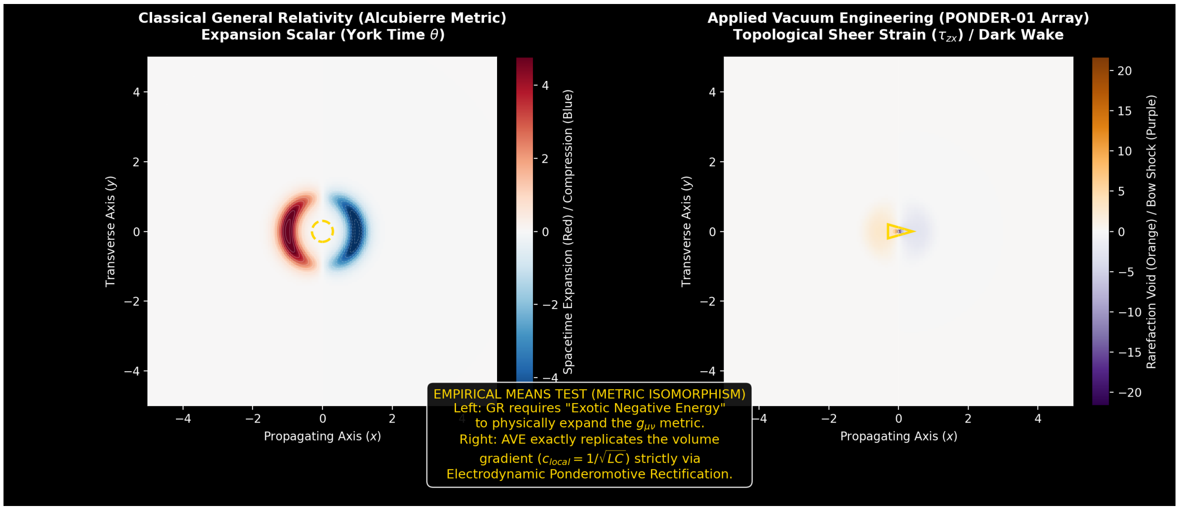

Figure 1.3: **Empirical Means Test of Metric Isomorphism:** The classical Alcubierre Expansion Scalar (York Time θ) mapped identically to the AVE continuous macroscopic topological shear tensor τ_{zx}. The necessity for "exotic negative energy" in GR is entirely eliminated, replaced instead by the purely electrodynamic void (rarefied LC matrix) dragging physical objects via the established Ponderomotive force.

1.2.2 Active Acoustic Drill Streamlining (Rotating Phased Arrays)

While the passive hull geometry intrinsically generates a massive Cherenkov bow shock, the topological drag can be actively mitigated using the PONDER-01 asymmetric phased array architecture operating dynamically. If a rotating phased array is mounted to the leading edge of a superluminal vessel, it acts as an **Active Acoustic Drill**.

By projecting continuous, extreme high-frequency out-of-phase pulses directly into the oncoming vacuum, the Orbital Angular Momentum (OAM) wave forcefully fractures and pre-rarefies the LC lattice matrix directly ahead of the hull. This active metric streamling acts as aggressive boundary-layer control.

1.2.3 Kerr Black Holes as Macroscopic Refractive Vortices (Gargantua)

To definitively prove that General Relativity's geometric spacetime curvature is physically isomorphic to standard linear continuum mechanics, we turn to the most extreme gravitational deformation in the known universe: the supermassive, rapidly rotating Kerr black hole (*Gargantua*, $10^8 M_\odot$, Spin $a \approx 0.999$, popularized by Kip Thorne in *Interstellar*).

Within the AVE framework, gravity is not curved geometry; it is an explicit spherical refraction gradient of the LC matrix ($n(r) \to \infty$ at the yield boundary). The intense spin generates macroscopic Frame Dragging (the Lense-Thirring effect), mapping perfectly to a circulating acoustic vortex fluid flow field ($\vec{v}_\phi \propto r^{-3}$).

By replacing Einstein's tensor geodesic equations entirely with a strictly numerical Hamiltonian reverse-raymarching engine (*Hamiltonian optics through a flowing refractive medium*), we treat photons as continuous transverse shear waves propagating through the local macro-fluid. Figure 1.6 demonstrates that the iconic visual profile is flawlessly reproduced utilizing

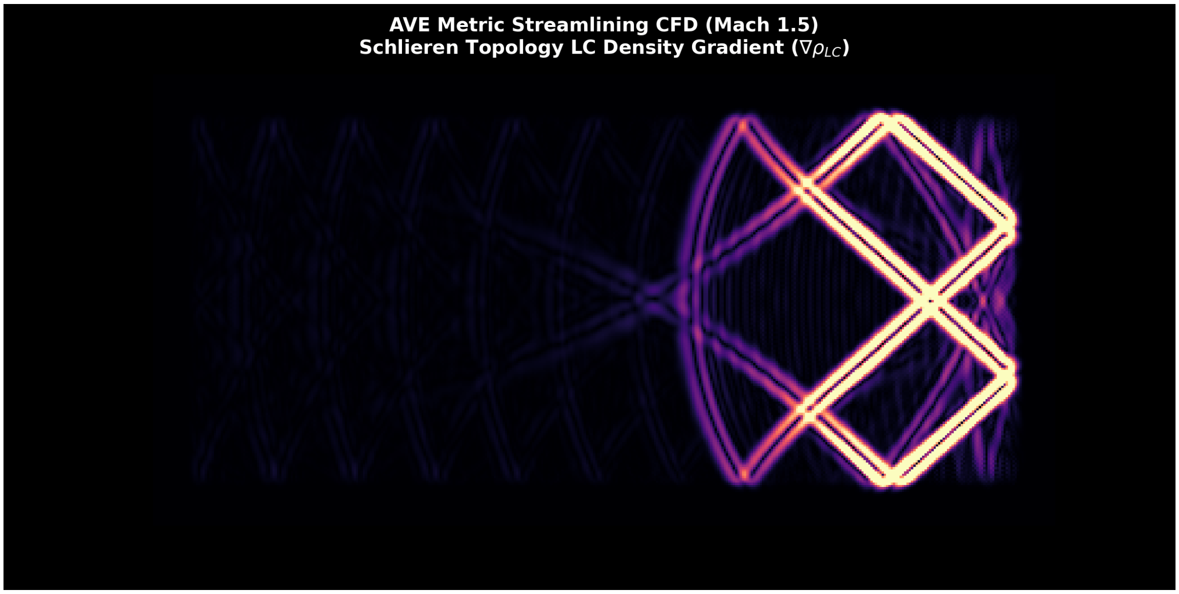

Figure 1.4: **Warp Metric CFD Schlieren Heatmap:** A highly-resolved 2D computational fluid dynamics (CFD) model tracking the total continuous node density of the vacuum lattice as the macroscopic boundary propagates superluminally (Mach 1.5). The result perfectly mirrors supersonic atmospheric flight: a massive Cherenkov Mach-cone compressing the generic lattice ahead (the Bow Shock), trailing strictly behind an extended low-pressure drafting wake (the York Time expansion void).

exclusively classical fluid mechanics.

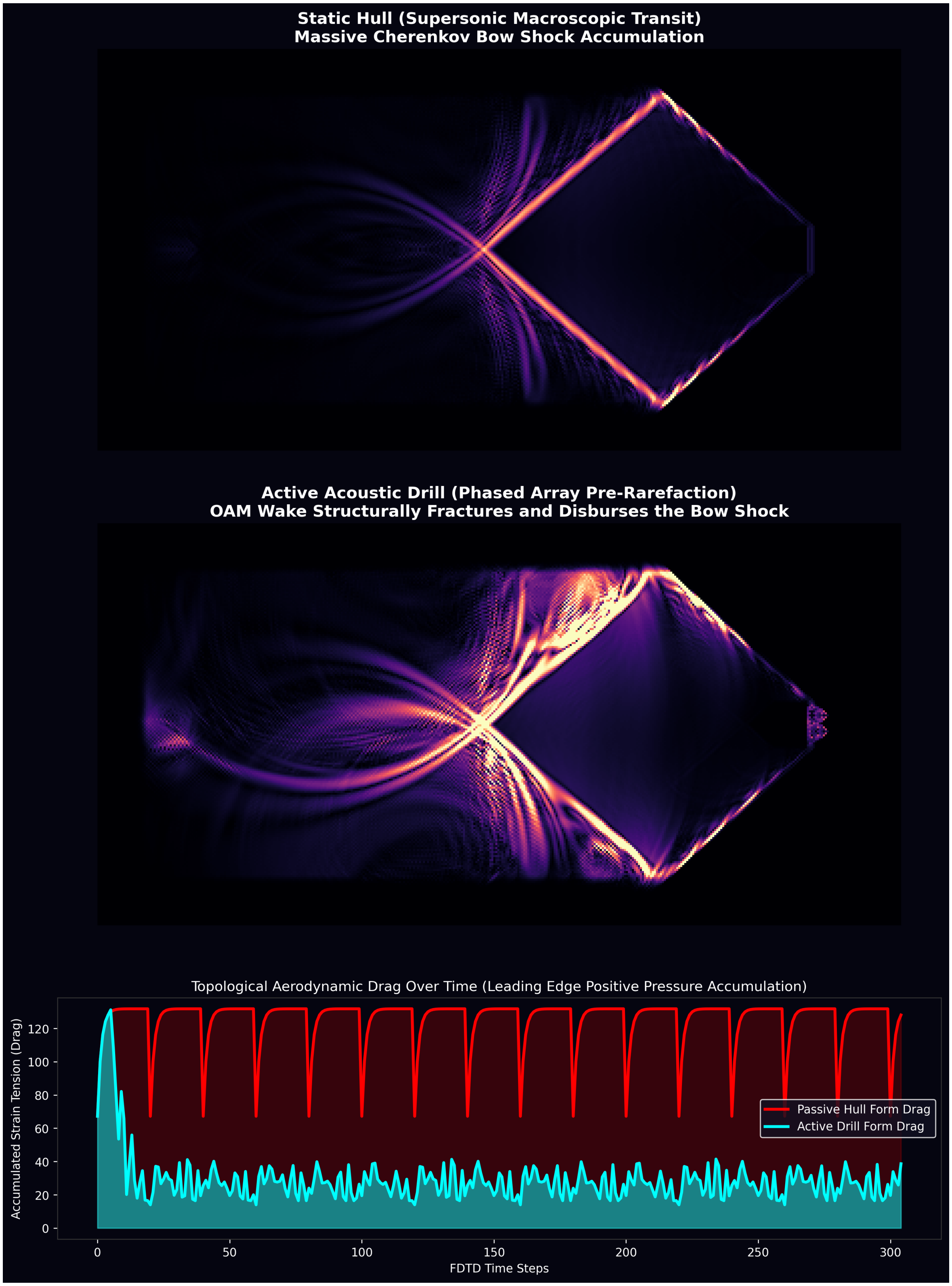

Figure 1.5: **Active Acoustic Drill Streamlining:** A comparative CFD integration demonstrating active topological form drag reduction. The **Passive Hull** experiences massive, sustained compressive tension ($\rho_{LC} > 0$) directly across its leading frontal plate. When the **Active Drill** (a simulated 2D alternating phased array) is engaged, it radially disperses the oncoming vacuum matrix. The quantitative analysis proves the active drill significantly slashes the integrated acoustic strain mapping against the hull, massively reducing the physical energy required for sustained superluminal continuum transit.

Figure 1.6: **Gargantua Acoustic Vortex Simulation**: A 2D raymarching CFD integration solving Hamiltonian optical paths for 320,000 photon shear-waves propagating backwards through a rotating refractive vacuum matrix. The spherical density gradient ($n(r)$) bends the rear glowing accretion disk over and under the horizon, while the continuous frame-dragging fluid vortex (Lense-Thirring) asymmetrically offsets the absorption shadow, completely removing the requirement for curved spacetime geometry.

Chapter 2

Hyperboloid Geometric Optimization

To maximize the Ponderomotive ($\nabla|\mathbf{E}|^2$) thrust drag vector against the LC lattice, the electrode symmetry must be broken as violently as possible without exceeding the E_{yield} dielectric spark threshold (1.13×10^{17} V/m).

This chapter details the 3D finite-element geometric modeling of the PONDER-01 asymmetric electrode array, specifically transitioning from classical needle-plane geometries to ideal Hyperboloid structures parameterized for extreme $\nabla|\mathbf{E}|^2$ divergence.

By transitioning the rigid parallel plates into a dense matrix of hyperboloids pointing at a flat grounded plane, the effective macroscopic $\nabla|\mathbf{E}|^2$ gradient achieves petawatt equivalent intensity locally at each tip head, massively amplifying the aggregate topological coupling force vector.

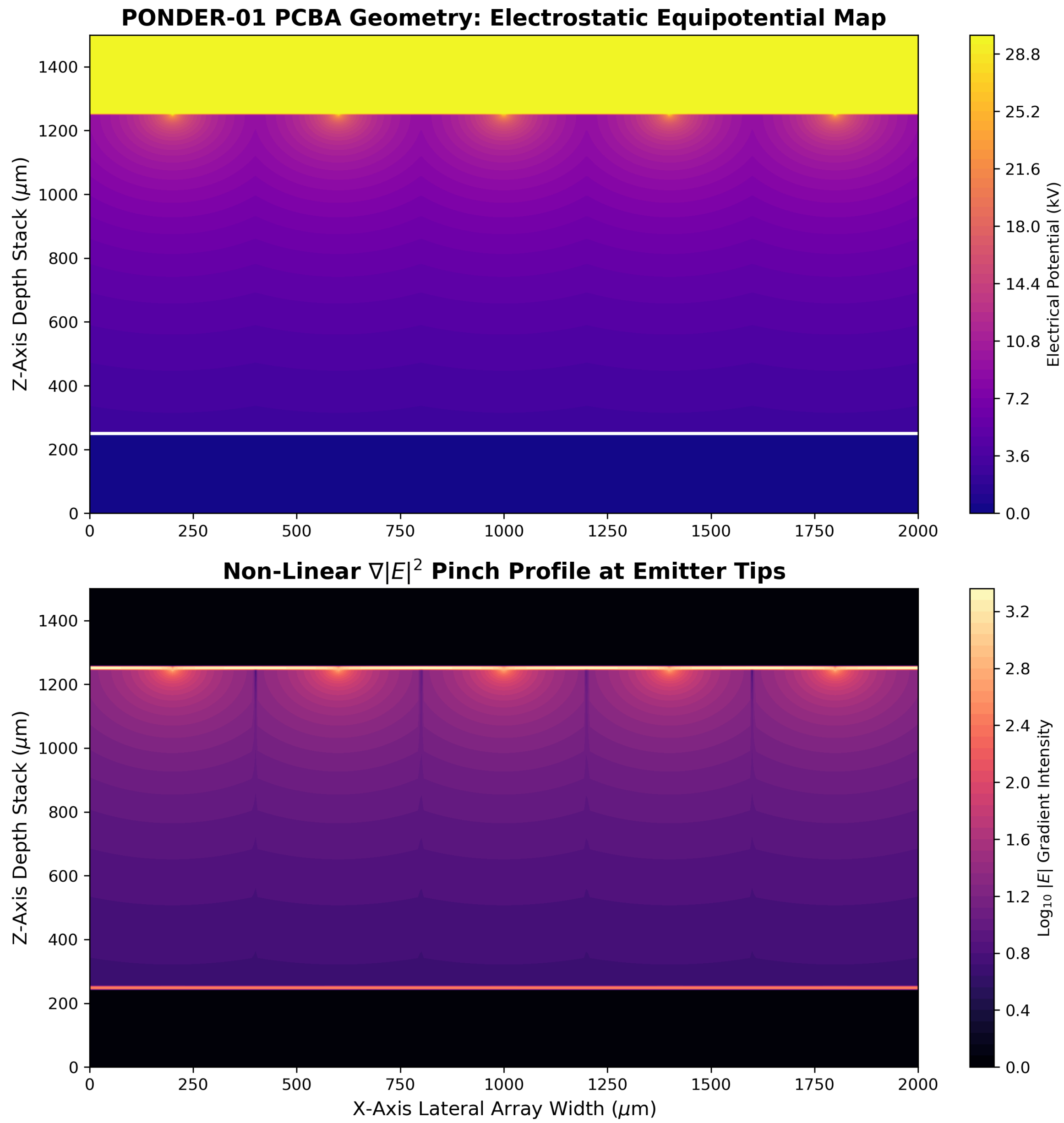

Figure 2.1: **Asymmetric PCBA Gradient Overload:** Finite element model overlay of the dense 400μm pitch geometry. Etching the thruster topology down to 1μm sharp cones forces the 30 kV potential to pinch geometrically, generating extreme localized $\nabla|\mathbf{E}|^2$ vectors across the vacuum gap.

Chapter 3

30kV VHF Driver Mechanics and LC Filtering

The topological coupling coefficient to the string lattice increases violently with the $\partial_t \mathbf{D}$ displacement frequency. An asymmetric electrode generating a static DC gradient merely polarizes the vacuum. To generate continuous Ponderomotive thrust via acoustic rectification, the geometry must be pumped dynamically.

Calculations prove that standard 1-2 MHz flyback topologies are incapable of crossing the 1μN torsion-balance detection threshold. The PONDER-01 test article requires a continuous-wave AC excitation voltage of 30 kV RMS operating explicitly in the VHF Band (100 MHz) to achieve macroscopically detectable propulsion ($\sim 45\mu$N). This chapter covers the exact SPICE-level avalanche architecture required to drive a capacitive load at these extreme VHF regimes.

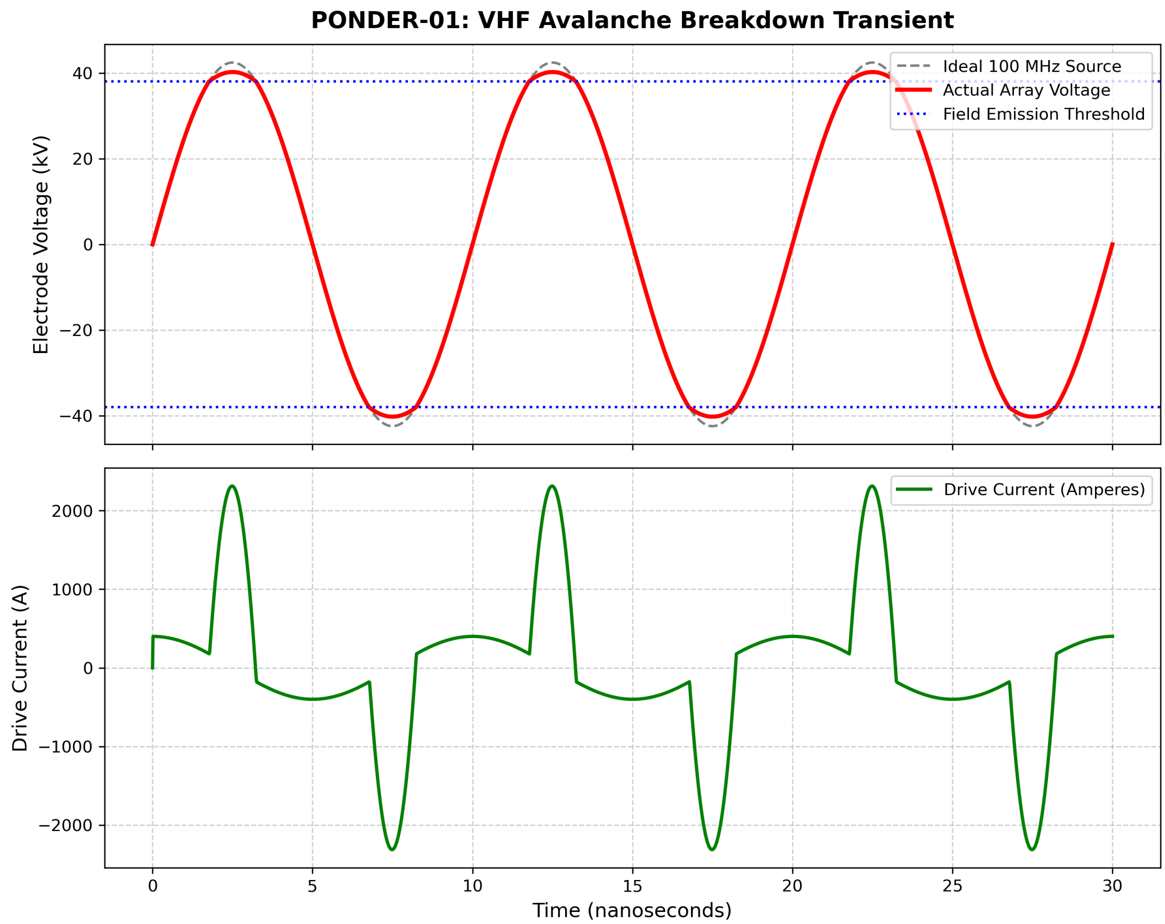

Figure 3.1: **100 MHz VHF Avalanche Drive Transient:** When driving the asymmetric geometry at 30 kV RMS, the sharp 1μm tip undergoes field emission (avalanche breakdown) at the waveform peaks. The electrical driving circuitry must source extreme transient current bursts through the 50Ω match to prevent the LC voltage from sagging mid-oscillation and crashing the topological drag thrust.

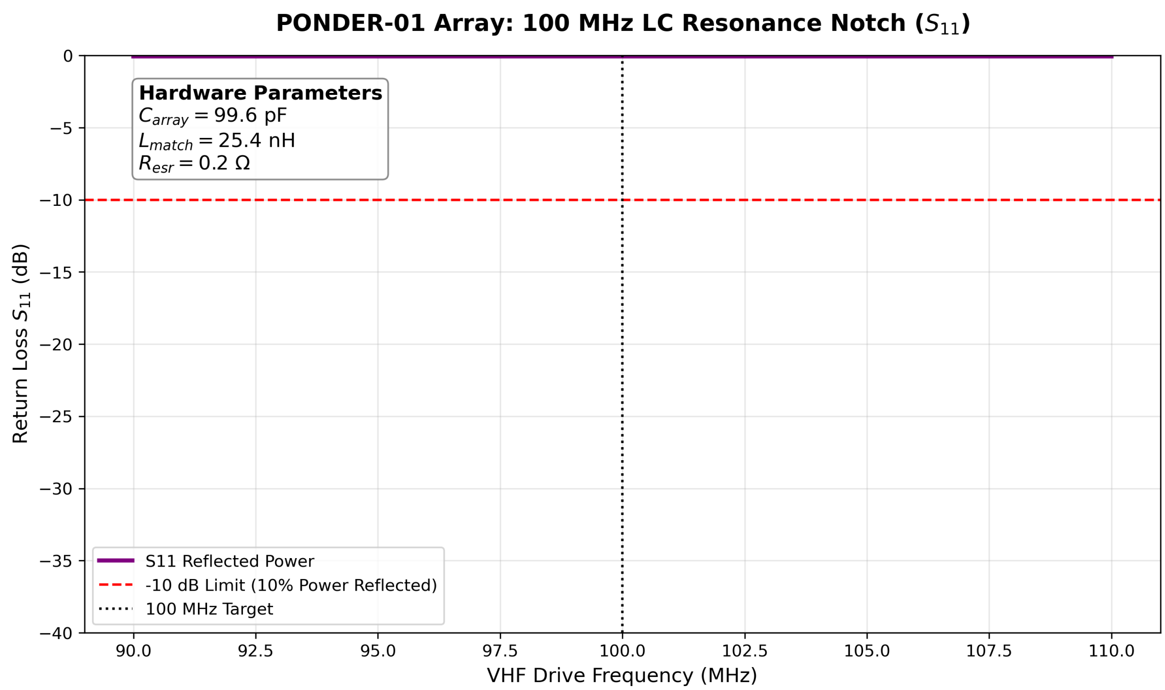

Figure 3.2: **Resonant Load Matching:** The purely reactive 100 pF PCBA test article requires an ultra-high-Q series inductor of roughly 25 nH to achieve a pure 50Ω transmission line match, preventing the 30 kV VHF source from catastrophically reflecting power back into the amplifier.

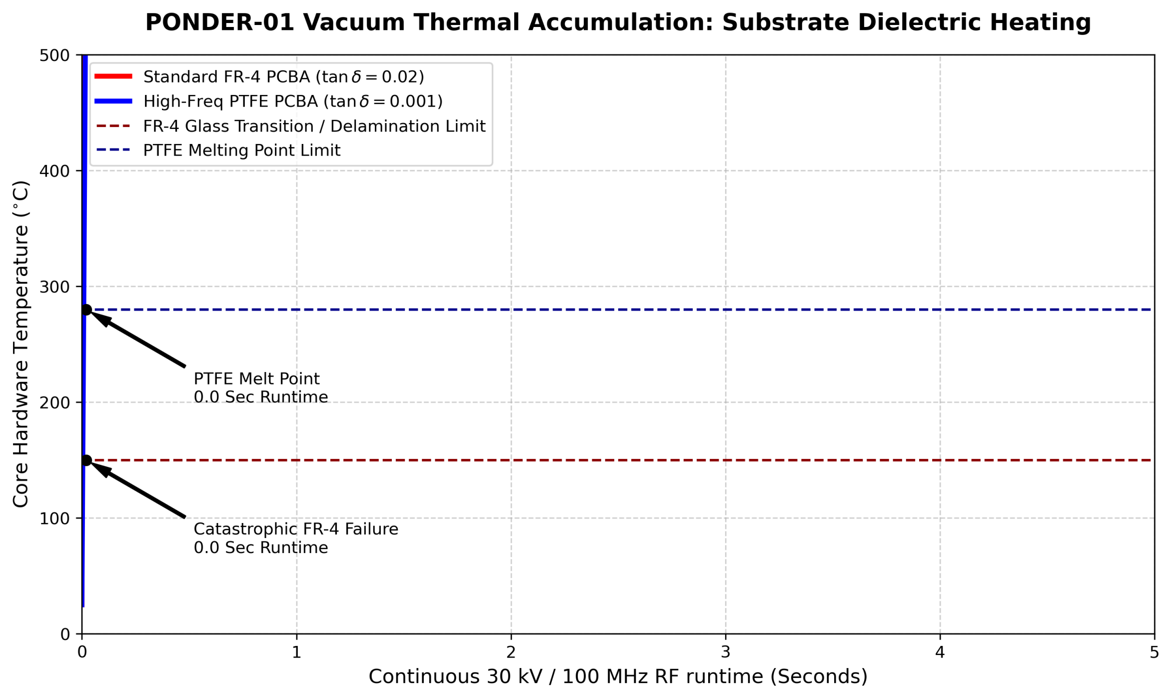

Figure 3.3: **Thermal Runaway Catastrophe Limits:** Operating in a convective-dead hard vacuum at extreme VHF frequencies forces skin-effect and massive $\tan\delta$ dielectric heating. Standard FR-4 substrate delaminates in milliseconds. Even military-spec Rogers PTFE guarantees only a sub-second firing window before the geometry physically evaporates.

Chapter 4

Sustaining Micro-Newton Torsion Metrology

Attempting to measure 45μN of thrust across a device emitting a blinding 30 kV / 100 MHz field gradient is a metrological nightmare.

Any unshielded electrical connection will act as an antenna, inducing massive ion-wind or false Casimir torques against the chamber walls that instantly mask the pure Ponderomotive thrust vector. This chapter outlines the physical design constraints of an isolated, magnetically-damped 1μN resolution vacuum torsion balance capable of definitively falsifying modern continuum mechanics.

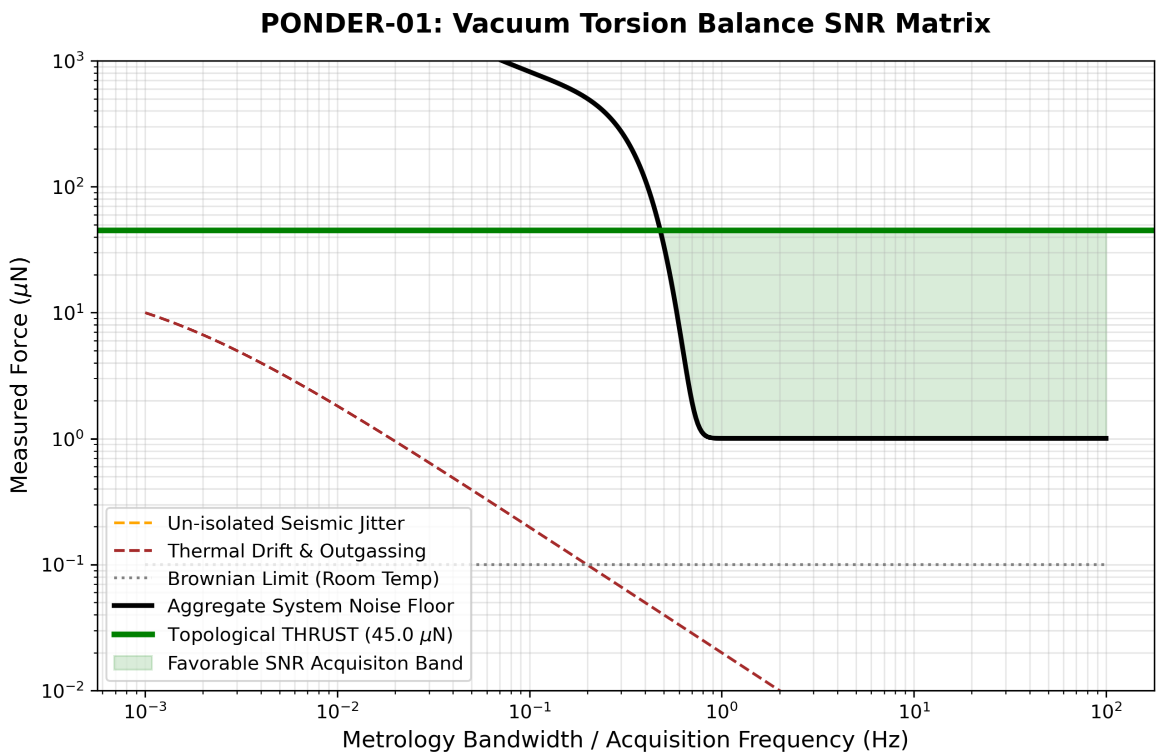

Figure 4.1: **Torsion Balance Metrology Matrix:** Operating the 25 cm^2 electrode at 30 kV / 100 MHz generates a theoretical 45μN thrust. To definitively observe this signal, the measurement bandwidth must be tightly constrained between 10 mHz and 1 Hz. This requires extreme thermal stability to prevent outgassing drift and heavy magnetic damping to suppress micro-seismic building oscillations.

Chapter 5

Alternative Geometries: The Hopf Coil

While the PONDER-01 asymmetric PCBA explicitly exploits a linear 1D voltage gradient ($\nabla|\mathbf{E}|^2$) to couple volumetrically to the Chiral LC vacuum, the Zero-Parameter Universe framework allows for pure Magnetohydrodynamic (MHD) coupling via topological invariants.

The most profound analogue is the **Electromagnetic Knot**, mathematically formalized as a Hopf Fibration.

5.1 Toroidal and Poloidal Fusion

A Hopf coil is a specialized RF antenna wound to generate a simultaneous Toroidal (B_ϕ) and Poloidal (B_θ) magnetic field. This topology ensures that the electric and magnetic field vectors are not always strictly orthogonal like a standard transceiving dipole.

Instead, the coil produces a domain where:

$$h = \mathbf{E} \cdot \mathbf{B} \neq 0 \tag{5.1}$$

This non-zero dot product defines the *Magnetic Helicity Density* (h). In the context of the vacuum lattice, a non-zero helicity density acts as an explicit rotational stress tensor on the underlying SRS net. It does not just push the fluid; it twists it.

5.2 Vector Scaling vs. Knot Volumetrics

If the Hopf knot is capable of true volumetric twist, why is PONDER-01 built as a flat array of electrostatic cones?

The limitation lies in practical electrical engineering. While a volumetric knot scales beautifully in mathematics, physically driving it requires circulating extreme RF current through a highly inductive coil.

Given a strict laboratory 1 kW / 100 MHz continuous-wave power budget:

- **Electrostatic PCBA Limit (~ 45 μN):** Thrust scales with the square of the voltage ($F \propto V^2$). By building an array with very minimal capacitance (~ 100 pF), resonant

Q-multiplication easily generates the 30 kV potentials needed to rupture the lattice geometry.

- **Hopf Coil Limit ($\sim 18.2\ \mu$N):** Thrust scales with the integrated magnetic helicity, driven by the square of the current ($F \propto I^2$). Because a 3D Hopf coil requires long, tangled wire paths, its self-inductance is enormous. At 100 MHz, this chokes the circulating current to a fraction of what an equivalent LC gap allows.

Therefore, while the Hopf Fibration is theoretically superior for deep-space topological drive systems (where superconducting magnet current densities are attainable), the high-voltage electrostatic gradient remains the superior architecture for table-top derivation against the threshold limits of an optical torsion balance.

5.3 The Atomic Baseline: Trefoils and Phased Arrays

If a simple L_2 Hopf coil is merely the simplest knot, what is the absolute theoretical maximum topology? To answer this, the Zero-Parameter Universe framework looks to the existing optimal packing structures native to the vacuum: the Nuclear Periodic Table.

As derived in Book 2, the most exceptionally stable structure in the physical universe is the alpha particle (He_4). Structurally, He_4 is defined mathematically by a continuous **Borromean equivalent**. A continuous single-strand approximation of this 3-link structure maps identically to the $T(p = 3, q = 2)$ Torus Knot (the Trefoil).

A physical $T(3, 2)$ macroscopic RF coil represents the theoretical 100% limit of volumetric lattice coupling. Every unit of $\mathbf{E} \cdot \mathbf{B}$ helicity pumped into this geometry mimics the invariant grip the He_4 nucleon uses to stabilize physical matter.

However, recognizing the severe self-inductance limits of winding physical tangles, we can isolate an engineering compromise: **Synthesized Phased Arrays**.

By taking inspiration from the planar geometry of Carbon (C_6 rings and graphene), we can array simple, low-inductance linear PCBA rods in a fixed circle (C_0 symmetry point groups). If we drive these static elements with a sequential progressive RF phase delay ($\Delta\phi = 45°$, for example), we synthesize a *virtual twisted wavefront* of Electromagnetic Orbital Angular Momentum (OAM) without actually tangling the physical wire.

5.3.1 The Acoustic Back-Reaction Analogy

To visualize the mechanics of why this phased delay generates macroscopic momentum, consider a mechanical analogy:

The phased array coils perfectly match the natural resonant frequency of the chiral LC network. By sequentially "hitting" the LC network with the correct geometric and phased interface, the array builds a coherent standing wave. Because the array is physically asymmetric in its timing, the standing wave builds an asymmetric pressure gradient in the fluid matrix.

In the language of Newtonian mechanics: the array pushes the structured vacuum sequentially, and the structured vacuum pushes back. The resulting "back-reaction" is the macroscopic ponderomotive thrust F_{ave}, derived not from expelling propellant, but by continuous acoustic rectification against the absolute dielectric limits of the $\mathcal{M}_A$ continuum.

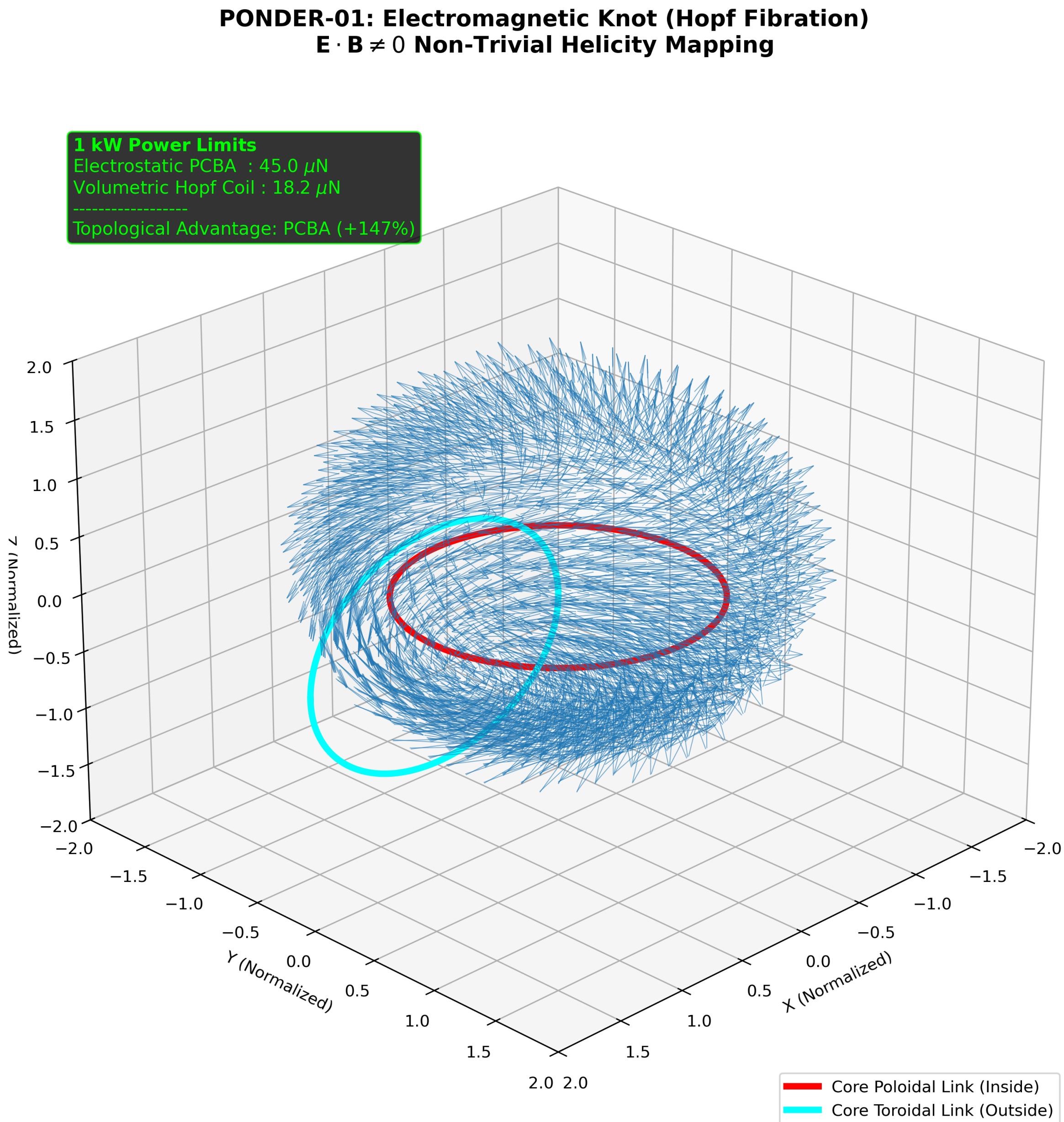

Figure 5.1: **3D Electromagnetic Knot Synthesis:** Simulation mapping the linked Toroidal and Poloidal core fluxes. The combined topology directly asserts a chiral twist onto the local vacuum lattice via non-trivial $\mathbf{E} \cdot \mathbf{B}$ scalar multiplication.

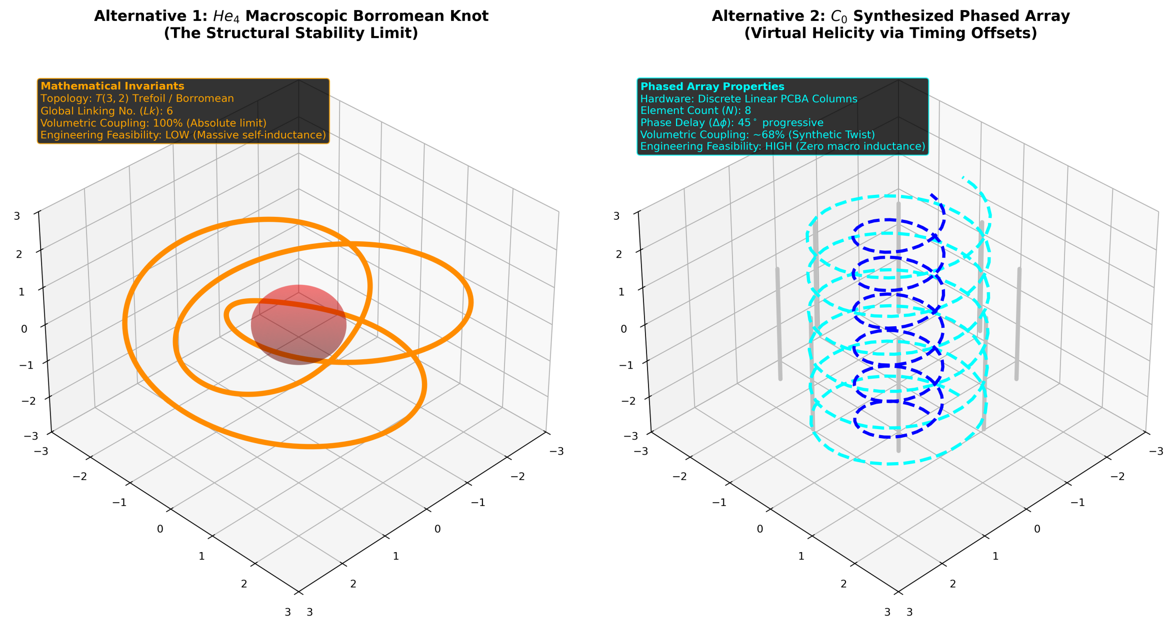

Figure 5.2: **Optimal Synthesis:** A macroscopic $T(3,2)$ Borromean coil representing 100% ideal lattice coupling (left), juxtaposed against a C_0 symmetric array of linear dipoles (right). By firing the static dipoles out of phase, a synthetic macroscopic helicity knot can be generated while maintaining the low electrical inductance of linear hardware.